



**HAL**  
open science

**Biomineralization at the Molecular Level: Amino  
Acid-Assisted Crystallization of Zeotype  
 $\text{AlPO}_4 \times 1.5\text{H}_2\text{O} - \text{H}_3$**

Qiaolin Lang, Guangying Fu, Haonuan Zhao, Juan Wang, Xiaobo Yang,  
Valentin Valtchev

► **To cite this version:**

Qiaolin Lang, Guangying Fu, Haonuan Zhao, Juan Wang, Xiaobo Yang, et al.. Biomineralization at the Molecular Level: Amino Acid-Assisted Crystallization of Zeotype  $\text{AlPO}_4 \times 1.5\text{H}_2\text{O} - \text{H}_3$ . *Crystal Growth & Design*, inPress, 10.1021/acs.cgd.1c01160 . hal-03429665

**HAL Id: hal-03429665**

**<https://hal.science/hal-03429665>**

Submitted on 15 Nov 2021

**HAL** is a multi-disciplinary open access archive for the deposit and dissemination of scientific research documents, whether they are published or not. The documents may come from teaching and research institutions in France or abroad, or from public or private research centers.

L'archive ouverte pluridisciplinaire **HAL**, est destinée au dépôt et à la diffusion de documents scientifiques de niveau recherche, publiés ou non, émanant des établissements d'enseignement et de recherche français ou étrangers, des laboratoires publics ou privés.

# Biom mineralization at a molecular level: Amino acid-assisted crystallization of zeotype $\text{AlPO}_4 \cdot 1.5\text{H}_2\text{O}\text{-H3}$ (APC)

Qiaolin Lang,<sup>1)</sup> Guangying Fu,<sup>1)</sup> Haonuan Zhao,<sup>1,2)</sup> Juan Wang,<sup>1)</sup> Xiaobo Yang,<sup>\*,1)</sup>  
Valentin Valtchev<sup>\*,1,2)</sup>

- 1) The ZeoMat Group, Qingdao Institute of Bioenergy and Bioprocess Technology, CAS, Laoshan District, CN-266101 Qingdao, China.
- 2) Normandie University, ENSICAEN, UNICAEN, CNRS, Laboratoire Catalyse et Spectrochimie, F-14000 Caen, France..

\* Corresponding authors: [yangxb@qibebt.ac.cn](mailto:yangxb@qibebt.ac.cn), [valentin.valtchev@ensicaen.fr](mailto:valentin.valtchev@ensicaen.fr)

**ABSTRACT:** Three amino acids: proline, histidine, and lysine are used as organic additives in the hydrothermal synthesis of the zeotype material  $\text{AlPO}_4 \cdot 1.5\text{H}_2\text{O}\text{-H3}$  (framework topology code **APC**). A detailed analysis of the factors controlling the formation of  $\text{AlPO}_4 \cdot 1.5\text{H}_2\text{O}\text{-H3}$  is performed. The role of amino acids in the formation process of the frameworks is addressed based on comparisons of the crystal phase selection of different synthetic recipes and the insights provided by the FTIR analysis of the synthetic gels and the crystalline products. The phase transition of  $\text{AlPO}_4 \cdot 1.5\text{H}_2\text{O}\text{-H3}$  to  $\text{AlPO}_4\text{-C}$  (**APC**), and subsequently to  $\text{AlPO}_4\text{-D}$  (**APD**) upon heating to 1000°C was followed by *in situ* XRD analysis. The present work has been the first progress to understanding the role of the bioactive molecules in the crystallization of inorganic open-framework microporous materials. An active, non-classical structure-directing role that amino acids play during the zeotype crystallization is proposed, i.e., positively charged amino acids cap the growing surface of microporous  $\text{AlPO}_4$ , and attract aluminate and phosphate anions from the solution phase for further growth.

## INTRODUCTION

Zeolites are tectosilicate materials defined by 4-connected framework structures with ring openings accessing intracrystalline void spaces.<sup>1</sup> Zeotype materials are extensions of zeolites, in the sense that the major framework building blocks, i.e.,  $\text{SiO}_4$ -tetrahedra, are partly or totally replaced by  $\text{PO}_4$ - or tetrahedra of other elements, while the 4-connected, crystalline, and microporous topologies are maintained.<sup>2</sup> In a wider extension, interrupted structures with building blocks other than just tetrahedra are also tolerated, and the framework material are still considered as zeotype.<sup>3</sup> Zeolites and zeotype materials have wide applications in the oil refineries and petrochemical industries as adsorbents and catalysts.<sup>3-5</sup> In recent years, new applications in renewable energies and environmental protection are explored and implemented.<sup>6-8</sup> Other technical exploits of zeotypes' specific chemical and surface properties in further advanced applications such as electronics, optics, medicine, etc., are investigated.<sup>9</sup>

A common method to synthesize zeolites and zeotype materials is hydrothermal crystallization, where hydrogels are prepared using precursor compounds for the framework building blocks and combined with

a mineralizer (either hydroxyl or a fluorine anion) in water; then, the crystallization of the targeted zeolite are carried out under autogenous steam pressures at elevated temperatures.<sup>10</sup> Often for high silica zeolites and for  $\text{AlPO}_4$  zeotypes in the hydrogel preparation step, organic ammonium, amine, phosphene, or another type of organic compound, is also added. This organic species works as a structure-directing agent (SDA), that governs or even determines the formation of the framework topology by interacting with the building block oxo-anions and directs their condensation to the targeted framework. In ideal cases, but not mandatory, SDA molecules/ions are occluded in the intra-crystalline void spaces of the product. The shape of the void cage/channel may even be an exact replica of the SDA shape. Then the SDA may be called template.<sup>11-12</sup> The broad choice of SDA types and structures has led to successful syntheses of many new zeolites. So far, 255 unique topologies of real existing materials have been approved by the International Zeolite Association on behalf of IUPAC; a majority of them are synthetic.<sup>13</sup> Yet, millions of energetically favored frameworks remain to be discovered or invented.<sup>14</sup>

However, it has been no report yet for the use of aminoacids as the SDA in the crystallization of zeolites and zeotype materials. The reason may be that in aqueous media, the carboxylic anions repulse the anionic building blocks of the framework materials, i.e., silicate, aluminate, and phosphate species, etc. Even if a zeolite synthesis is carried out in the presence of aminoacids, these bioactive molecules are hardly involved in the crystallization process of those oxo-anions. Syntheses of a hierarchical **LTA** zeolite has been successful with various aminoacids as mesoporogens.<sup>15-16</sup> Hierarchical **FAU** zeolite have been obtained as well with aminoacids as mesoporogens.<sup>17</sup> Our previous study on the roles of aminoacids and low peptides in the crystallization of **MFI**-type zeolites reveals that these organic species work as diffusion modifiers, affects the system rheology, thus have impacts on the crystal morphology of the products.

Nevertheless, further attempts to use aminoacids as SDA for zeolites are worthy because, upon success, it would bridge bio-organic chemistry and inorganic microporous materials. Considering the great structural variety of aminoacids, and the versatility of inorganic oxo-anions as building blocks, many chemical and structural combinations of aminoacids and framework topologies would come into account, which would open a vast chemical field for discoveries of materials with new properties.

A further expectable advance to use aminoacids as SDA in the zeolite crystallization is that the chirality of aminoacid molecules may be translated into the porosity of the crystalline products, besides their shape and sizes. The synthesis of a chiral molecular sieve has been a long-standing goal in the field of zeolites.<sup>18</sup> And first successful examples emerge in recent years. Chiral molecular sieves are expected to be applicable as heterogeneous catalysts and adsorbents, which would be a game-changer in the pharmaceutical industry.<sup>19-21</sup> The series of zincophosphate materials crystallized at the presence of d-glucosamine with various structural and porous properties inspire translating the chirality of a bioactive molecule to inorganic porous crystals.<sup>22</sup>

An interaction of aminoacids with zeolite frameworks may be established when the organic moiety becomes positively charged.<sup>23-24</sup> The present paper introduces a strategy to overcome the repulse between the carboxylic anions and the anionic building blocks: carboxylic anion is capped with methanol to form a

methyl ester, and the crystallization of zeolites or zeotypes is performed in acidic media, where the amino groups of the SDA become protonated and positively charged. Therefore, an affinity between the SDA and the inorganic anions is built up. It enables condensations of inorganic anions in the vicinity of the aminoacid, leading to nucleation and crystal growth.

The present paper is to demonstrate that the first success of the above strategy has been achieved in the synthesis of the zeotype  $\text{AlPO}_4 \cdot 1.5\text{H}_2\text{O} \cdot \text{H}_3$  (Framework topology code **APC**) at the presence of proline, histidine, or lysine, at various temperatures and concentrations. In addition, a few other non-zeolitic framework  $\text{AlPO}_4$  materials have been observed to crystallize at the presence of the aminoacids, including  $\text{AlPO}_4 \cdot \text{H}_2\text{O} \cdot \text{H}_4$ , variscite,  $\text{AlPO}_4$ -cristobalite, etc. Although  $\text{AlPO}_4 \cdot 1.5\text{H}_2\text{O} \cdot \text{H}_3$  (**APC**) is a long-known structure, the successful crystallization with aminoacids as SDA demonstrates the first leap towards further discoveries in the new field. We may consider the aminoacids-assisted crystallization of  $\text{AlPO}_4$  compounds as a type of biomineralization at the molecular level, in addition to the formation of structured inorganic functional materials at meso- and macro-scales with aids of organisms.<sup>25</sup>

In the paper, the conditions of crystallizations of  $\text{AlPO}_4 \cdot \text{H}_2\text{O} \cdot \text{H}_3$  (**APC**) and the other framework  $\text{AlPO}_4$ s are elaborated; the products are characterized; and above all, the role of aminoacids during the crystallization is proved and discussed based on comparisons of the crystal phase selections of various synthetic recipes, and based on FTIR studies that track down the synthetic gels and the crystalline products.

## EXPERIMENTAL SECTION

**Materials.** L-proline methyl ester hydrochloride (Pro-OMe·HCl, 98%), L-histidine methyl ester dihydrochloride (His-OMe·2HCl, 98%), L-lysine methyl ester dihydrochloride (Lys-OMe·2HCl, 98%), aluminum iso-propoxide ( $\text{Al}(\text{OPr})_3$ , analytical purity) were purchased from Macklin. Phosphoric acid (85%) was from Sigma-Aldrich. Deionized water was used throughout the experiments.

**Hydrothermal Synthesis.** A common recipe of the molar ratios 1 AA: 1  $\text{Al}(\text{OPr})_3$ : 1  $\text{H}_3\text{PO}_4$ : x  $\text{H}_2\text{O}$  was used to prepare the initial hydrogel. AA stands for above-mentioned aminoacids ester hydrochloride salts. And x was varied as 34, 67 and 130, respectively. In addition, a series of blank control experiments have been carried out with the gel composition (0, 1 and 2) HCl: 1  $\text{Al}(\text{OPr})_3$ : 1  $\text{H}_3\text{PO}_4$ : 67  $\text{H}_2\text{O}$ .

For the gel preparation, the calculated amount of AA was dissolved in  $\text{H}_2\text{O}$ .  $\text{H}_3\text{PO}_4$  and  $\text{Al}(\text{OPr})_3$  were then added consecutively under stirring. The stirring at room temperature was then continued for 24 hours. The gel became a semitranslucent and homogeneous fluid upon hydrolysis of  $\text{Al}(\text{OPr})_3$ .

A portion of the gel was centrifuged at 30.000 rpm for 60 min. The pH value of the liquid was recorded using a pH meter. Then the liquid supernatant and the sediment were freeze-dried separately. The sediments were washed twice with plenty of water before drying. Both the liquids and solids were subjected to spectroscopic characterizations.

The homogenized gel was sealed in a Teflon-lined autoclave and hydrothermally treated at 100, 120 and

140°C, for 24 hours to 21 days. Then the autoclave was quenched in cold water. The solid product was recovered, washed with plenty water, and dried at 80°C.

Table S1 in the Supporting Information is the complete list of synthetic experiments carried out and discussed in the present work.

**Characterization.** Powder X-ray diffraction was performed on a Rigaku SmartLab 9KW diffractometer using Cu K $\alpha$  radiation at 40 kV and 150 mA. 1D detector was used to collect diffraction data in a continuous scan mode in theta-theta geometry. High-temperature in situ XRD was carried out on the same diffractometer with Reactor-X cell, which has a Si sample holder in a heated chamber with a window made of Be foil. XRD patterns of selected samples were taken along a heating program at 10°C/min heating rate at 50°C steps up to 1000°C. At each step, the temperature was held for 5 min for XRD recording.

SEM pictures of powder samples were taken on JEOL JSM 7900F Scanning Electron Microscope equipped with a field emission gun operating at 2 kV. The samples were dusted on carbon tapes and inspected without coating.

<sup>27</sup>Al MAS NMR experiments were performed on Bruker AVANCE III 600 spectrometer equipped with a 4 mm triple resonance probe operating at a resonance frequency of 156.4 MHz. The spectra were recorded using a small-flip angle technique with a pulse length of 0.5  $\mu$ s ( $<\pi/12$ ) and a 1s recycle delay, and a spinning rate of 14 kHz. The chemical shifts of <sup>27</sup>Al were referenced to 1 mol/L aqueous Al(NO<sub>3</sub>)<sub>3</sub>.

<sup>31</sup>P MAS NMR experiments were carried out on a Bruker AVANCE III 600 spectrometer at a resonance frequency of 242.9 MHz using a 4 mm HX double-resonance MAS probe at a sample spinning rate of 12 kHz. Single-pulse <sup>31</sup>P MAS NMR experiments with <sup>1</sup>H decoupling were performed with a 90° pulse width of 3.2  $\mu$ s and a 180 s recycle delay, and a 1H decoupling strength of 80 kHz and 160 scans. The chemical shift of <sup>31</sup>P was externally referenced to 85% H<sub>3</sub>PO<sub>4</sub>.

FTIR spectra were recorded upon KBr pellets using Bruker Vertex 70V Spectrometer at a spectral resolution of 4 cm<sup>-1</sup>. The equipment, including the sample chamber, was evacuated to below 1 hPa.

TG/DTA analysis was performed using Rigaku TG-DTA8122 microbalance upon ca. 10 mg zeolite powder against  $\alpha$ -Al<sub>2</sub>O<sub>3</sub>, in 30 ml/min reconstituted airflow at a heating rate of 10°C/min.

## RESULTS AND DISCUSSION

**Brief descriptions of the aminoacids and the structures of the AlPO<sub>4</sub> products.** Three different aminoacids have been chosen for the investigation. They have various characters respecting the side chains (Chart 1). Proline is a smaller molecule, with the  $\alpha$ -amino group in the pyrrolidine ring having an pK<sub>a</sub> of 10.60. Histidine molecule has an imidazole ring at the end of the chain. The pK<sub>a</sub> of the  $\alpha$ -amino group is 9.17, of the ones in the imidazole ring is 6.00. Lysine has a similar size as histidine. There is a 6-carbon straight chain with 2 amino groups at the  $\alpha$ - and the  $\omega$ -positions. The pK<sub>a</sub> values of the amino

groups are 8.90 and 10.28, respectively. The carboxylic groups of the three molecules have similar  $pK_a$  values around 2.<sup>26</sup>

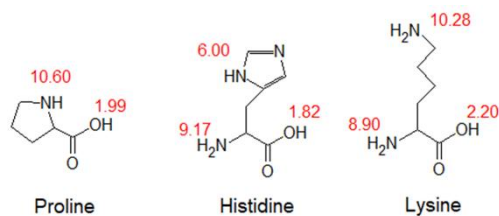


**Chart 1:** The three aminoacids used in the crystallization of framework  $AlPO_4$ s. Red numbers denotes the  $pK_a$  values of

In the zeolite synthesis, SDA needs to be positively charged. A possible strategy is to cap the carboxylic groups by making an ester and use it below the  $pK_a$  value of the amino groups. Methyl esters of these reagents are available as HCl salts, i.e., L-lysine methyl ester dihydrochloride (Lys-OMe·2HCl), L-histidine methyl ester dihydrochloride (His-OMe·2HCl), and L-proline methyl ester hydrochloride (Pro-OMe·HCl). In aqueous solutions, they can present as cations, with the amino groups being protonated when the solution pH is below the  $pK_a$  value of the respective amino group. This is the case of the experiments in the present work.

At the presence of the three aminoacid esters in the synthetic gels,  $AlPO_4 \cdot 1.5H_2O \cdot H_3$  (**APC**) crystals have been repeatedly obtained. A few other crystalline  $AlPO_4$  phases have been observed, too, at varying conditions. Brief descriptions of the structures are given here before the discussions on their formation conditions.

$AlPO_4 \cdot 1.5H_2O \cdot H_3$  is the hydrated form of zeolite  $AlPO_4$ -C (**APC**). **APC** is a 4-connected framework with 2-dimensional channels of 8-rings along [100] and [001] directions (Chart 2). The framework is composed of alternating  $AlO_4$ - and  $PO_4$ -tetrahedra. In the hydrated  $AlPO_4 \cdot 1.5H_2O \cdot H_3$ , however, Al2 bonds with two additional  $H_2O$  molecules, and become a 6-coordinated  $AlO_4(H_2O)_2$ -octahedron. Stoichiometrically, there is one more  $H_2O$  molecule that resides in the [001] channel at an ordered position via hydrogen bond.<sup>27-28</sup>

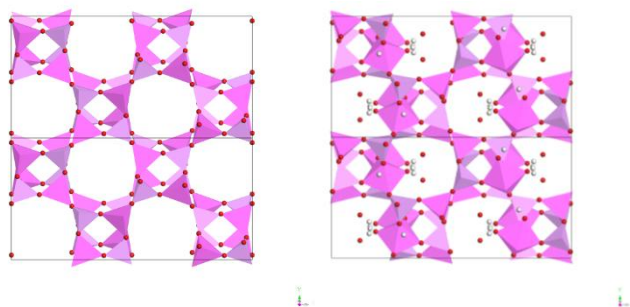


**Chart 2:** **APC** framework (left) and its hydrated form  $AlPO_4 \cdot 1.5H_2O \cdot H_3$  (right). In the hydrated form, Al2 coordinates to 2 additional  $H_2O$  molecules and become octahedra. Another  $H_2O$  molecule resides in the 8-ring channel.

$\text{AlPO}_4 \cdot \text{H}_2\text{O} \cdot \text{H}_4$  is a framework  $\text{AlPO}_4$  compound with 4-connected  $\text{PO}_4$ -tetrahedra connecting alternately to  $\text{AlO}_4$ -tetrahedra and  $\text{AlO}_4(\text{H}_2\text{O})_2$ -octahedra. Each  $\text{AlO}_4(\text{H}_2\text{O})_2$ -octahedron connects with four  $\text{PO}_4$ - and two  $\text{H}_2\text{O}$ . There are slit-shaped 8-ring channels approximately along [110], but they are too narrow to enable passages of any guest molecule (Chart 3).<sup>29</sup> Variscite is another observed framework with alternating tetrahedra-octahedra possessing 8-ring channels, which are blocked by the crystalline water (Chart 3).<sup>30</sup>

Besides the above hydrated  $\text{AlPO}_4$  framework materials,  $\text{AlPO}_4$ -cristobalite and another dense  $\text{AlPO}_4$ , which was previously observed but not characterized by d'Yvoire<sup>31</sup> and other authors, have been obtained in the aminoacids directed experiments, as well. The conditions that each phase forms are elaborated on below.

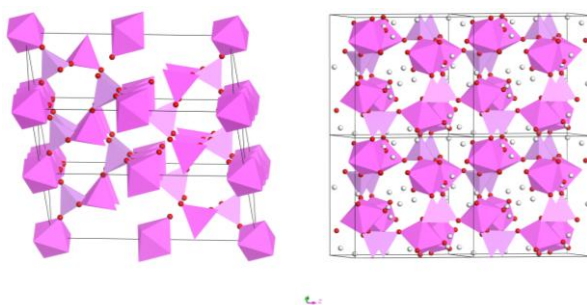


**Chart 3:** The framework of  $\text{AlPO}_4 \cdot \text{H}_2\text{O} \cdot \text{H}_4$  which has connections of alternating  $\text{AlO}_4$ - and  $\text{AlO}_4(\text{H}_2\text{O})_2$ - to  $\text{PO}_4$ -units, and 8-ring channels (left); and variscite with  $\text{AlO}_4(\text{H}_2\text{O})_2$ - connecting to  $\text{PO}_4$  forming 8-ring channels

**Crystallization condition** (right).

relatively simple. As in Ta... a pH value of 1.97. At this pH the pyrrolidine ring is protonated.

ents with proline appears  
)Pr)<sub>3</sub>: H<sub>3</sub>PO<sub>4</sub>: 67H<sub>2</sub>O has

Upon a hydrothermal treatment at 120°C, weak diffraction peaks of  $\text{AlPO}_4$ -cristobalite appear in 1 day. In 2 days,  $\text{AlPO}_4$ -cristobalite and  $\text{AlPO}_4 \cdot 1.5\text{H}_2\text{O} \cdot \text{H}_3$  (**APC**) coexist. The mixture transforms into pure and well-crystallized  $\text{AlPO}_4 \cdot 1.5\text{H}_2\text{O} \cdot \text{H}_3$  in 6 days. At a more severe condition, at 140°C in 21 days, the product remains crystalline  $\text{AlPO}_4 \cdot 1.5\text{H}_2\text{O} \cdot \text{H}_3$  (**APC**), with some  $\text{AlPO}_4 \cdot \text{H}_2\text{O} \cdot \text{H}_4$  impurity. For comparison, the gel became white at 100°C in 6 days, but the solid recoverable by high-speed centrifuge is X-ray amorphous.

Varying water dilution, the gel Pro-OMe·HCl:  $\text{Al}(\text{OPr})_3$ :  $\text{H}_3\text{PO}_4$ : 130H<sub>2</sub>O has a pH of 2.37. It crystallizes to  $\text{AlPO}_4 \cdot \text{H}_2\text{O} \cdot \text{H}_4$  at 120°C in 6 days, with a small amount of  $\text{AlPO}_4$ -cristobalite impurity. And, the gel Pro-OMe·HCl:  $\text{Al}(\text{OPr})_3$ :  $\text{H}_3\text{PO}_4$ : 34H<sub>2</sub>O has a pH of 2.58.  $\text{AlPO}_4 \cdot 1.5\text{H}_2\text{O} \cdot \text{H}_3$  (**APC**) starts to crystallize at 120°C in 6 days, but with  $\text{AlPO}_4$ -cristobalite as the main phase in the product.

Figure 1 shows the powder XRD patterns of the products. In general, middle to a low degree of dilution and low pH favor the formation of the open framework product **APC**, in the presence of protonated

proline.

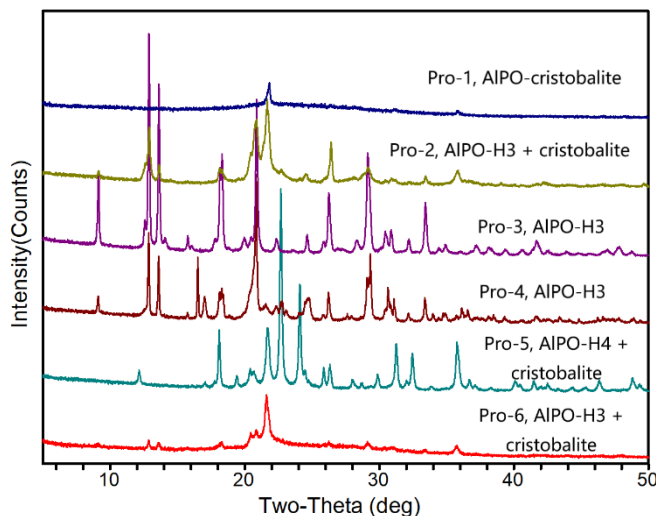


**Figure 1.** XRD patterns of the products at the presence of Pro-OMe-HCl.

From top to bottom, the patterns correspond the Exp# Pro-1 to Pro-6 in

The experiments with Table S1.

otherwise the same conditions. The initial gel of the composition His-OMe·2HCl: Al(OPr)<sub>3</sub>: H<sub>3</sub>PO<sub>4</sub>: 6/H<sub>2</sub>O has a pH of 1.88. At 120°C, it remains amorphous in 1 and 2 days. In 6 days, AlPO<sub>4</sub>·H<sub>2</sub>O-H4 crystallizes, with negligible AlPO<sub>4</sub>·1.5H<sub>2</sub>O-H3 (APC) impurity. At 140°C, it becomes pure AlPO<sub>4</sub>·H<sub>2</sub>O-H4 in 21 days. And it does not crystallize at 100°C in 7 days. Altering the water additions in the gels, His-OMe·2HCl: Al(OPr)<sub>3</sub>: H<sub>3</sub>PO<sub>4</sub>: 130 H<sub>2</sub>O has a pH value of 2.52, which is still far below the pK<sub>a</sub> of the α-amino group and the ones in the imidazole ring. It crystallizes into AlPO<sub>4</sub>·1.5H<sub>2</sub>O-H3 (APC) at 120°C in 6 days. His-OMe·2HCl: Al(OPr)<sub>3</sub>: H<sub>3</sub>PO<sub>4</sub>: 34 H<sub>2</sub>O has a pH of 2.22. It crystallizes into AlPO<sub>4</sub>·1.5H<sub>2</sub>O-H3 at 120°C in 6 days, too. Apparently, in the system with histidine the product selection is rather sensitive to pH value but not to water amount. Figure S1 in the Supplementary Information shows the XRD patterns of the crystals.

The product phase selection in the system with lysine is more complicated than using proline and histidine. The gel Lys-OMe·2HCl: Al(OPr)<sub>3</sub>: H<sub>3</sub>PO<sub>4</sub>: 67H<sub>2</sub>O has a pH of 1.95. At 120°C in 1 day, AlPO<sub>4</sub>·H<sub>2</sub>O-H4 starts to appear. In 2 days, the main product is AlPO<sub>4</sub>-cristobalite of low crystallinity. Then, in 6 days, another AlPO<sub>4</sub> product crystallizes in high purity and crystallinity. This phase has been observed but not fully characterized by d'Yvoire in 1961 (PDF 14-0329).<sup>31</sup> At the extreme condition at 140°C in 21 days AlPO<sub>4</sub>·H<sub>2</sub>O-H4 is well crystallized. And, at 100°C in 6 days, the product is amorphous.

Similar to the proline- and histidine-containing systems, varying the water content of the gel led to slightly higher pH values. Then the zeolitic phase AlPO<sub>4</sub>·1.5H<sub>2</sub>O-H3 (APC) crystallizes, but together with AlPO<sub>4</sub>·H<sub>2</sub>O-H4 from the gel Lys-OMe·2HCl: Al(OPr)<sub>3</sub>: H<sub>3</sub>PO<sub>4</sub>: 130H<sub>2</sub>O of pH = 2.44 at 120°C in 6 days; AlPO<sub>4</sub>·1.5H<sub>2</sub>O-H3 (APC) crystallizes as the single and pure product from the gel Lys-OMe·2HCl: Al(OPr)<sub>3</sub>: H<sub>3</sub>PO<sub>4</sub>: 34H<sub>2</sub>O of pH = 2.54 at 120°C in 6 days. XRD patterns of corresponding crystalline

with  $\text{AlPO}_4 \cdot \text{H}_2\text{O} \cdot \text{H}_4$  from the gel Lys-OMe $\cdot$ 2HCl:  $\text{Al}(\text{OPr})_3$ :  $\text{H}_3\text{PO}_4$ :  $130\text{H}_2\text{O}$  of pH = 2.44 at  $120^\circ\text{C}$  in 6 days;  $\text{AlPO}_4 \cdot 1.5\text{H}_2\text{O} \cdot \text{H}_3$  (APC) crystallizes as the single and pure product from the gel Lys-OMe $\cdot$ 2HCl:  $\text{Al}(\text{OPr})_3$ :  $\text{H}_3\text{PO}_4$ :  $34\text{H}_2\text{O}$  of pH = 2.54 at  $120^\circ\text{C}$  in 6 days. XRD patterns of corresponding crystalline products are presented in Figure S2.

Three blank control experiments have been carried out, without aminoacids, but with different amounts of HCl in the starting gels, to mimic the conditions with the aminoacids. At pH = 2.26 without HCl, the  $\text{AlPO}_4$  gel crystallizes rapidly into  $\text{AlPO}_4 \cdot \text{H}_2\text{O} \cdot \text{H}_4$  in 1 day at  $120^\circ\text{C}$ . With 1 molar equivalent HCl, to compare with Pro-OMe $\cdot$ HCl, the gel has a pH of 1.71, and the crystallization becomes so slow that a separation of solid/liquid does not even complete in 21 days at  $120^\circ\text{C}$ . The recoverable solid in 21 days is a mixture of  $\text{AlPO}_4 \cdot \text{H}_2\text{O} \cdot \text{H}_4$  and variscite. At a lower pH of 1.41 with 2 HCl, the crystallization is also slow, and the 21-day product is pure variscite. XRD patterns are in Figure S3.

These experiments imply that the crystalline phase of the product without aminoacids and with different kinds of aminoacids are not identical at otherwise same gel compositions and similar pH. Hence, the three aminoacids esters indeed play different roles in determining the crystalline product.

**Properties of  $\text{AlPO}_4 \cdot 1.5\text{H}_2\text{O} \cdot \text{H}_3$  (APC) and  $\text{AlPO}_4 \cdot \text{H}_2\text{O} \cdot \text{H}_4$  obtained with aminoacids.** The SEM pictures in Figure 2 show that  $\text{AlPO}_4 \cdot 1.5\text{H}_2\text{O} \cdot \text{H}_3$  (APC) obtained using the three different aminoacids have different sizes and shapes. All three samples appear to be irregular agglomerates of smaller crystallites. The primary crystallites obtained at the presence of proline are of sub-micron sizes and do not have a distinctive shape. The primary crystals with histidine are rod-like, with lengths of up to  $10 \mu\text{m}$ . The lysine-assisted crystals are rods of  $1\text{-}2 \mu\text{m}$ .

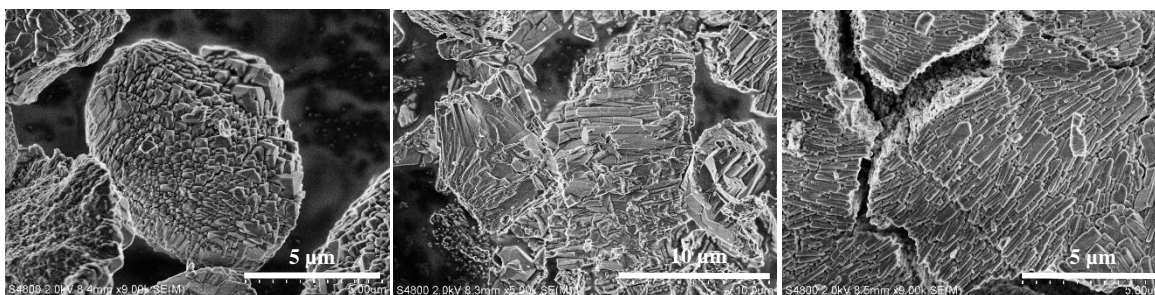


**Figure 2.** SEM pictures of  $\text{AlPO}_4 \cdot 1.5\text{H}_2\text{O} \cdot \text{H}_3$  (APC) crystallized at the presence of Pro-OMe $\cdot$ HCl, His-OMe $\cdot$ 2HCl, and Lys-OMe $\cdot$ 2HCl, respectively.

SEM of  $\text{AlPO}_4 \cdot \text{H}_2\text{O} \cdot \text{H}_4$  crystallized with His-OMe $\cdot$ 2HCl and Lys-OMe $\cdot$ 2HCl are shown in Figure S4. Both are seen as loose agglomerated plate-like primary crystals. Those plates are truncated bi-pyramids with small heights. The histidine-made crystals have edges of around  $3 \mu\text{m}$ , and thickness of  $0.5\text{-}1.0 \mu\text{m}$ . The lysin-assisted crystals have similar edges around  $3 \mu\text{m}$ , but they are  $1.0\text{-}3.0 \mu\text{m}$  thick. A pure  $\text{AlPO}_4 \cdot \text{H}_2\text{O} \cdot \text{H}_4$  has not been obtained at the presence of proline.

Figure 3 shows  $^{31}\text{P}$  MAS NMR and  $^{27}\text{Al}$  MAS NMR of two selected samples, i.e., Lys-6  $\text{AlPO}_4 \cdot 1.5\text{H}_2\text{O}$

H3 (**APC**) and Lys-4  $\text{AlPO}_4 \cdot \text{H}_2\text{O} \cdot \text{H}_4$ , both synthesized using Lys-OMe $\cdot$ 2HCl as SDA. The  $^{31}\text{P}$  MAS NMR spectrum of Lys-6 has two well-resolved resonance peaks for tetrahedrally coordinated P at  $\delta = -22$  and  $-26$  ppm, corresponding to P atoms at two distinct crystallographic positions in the orthorhombic unit

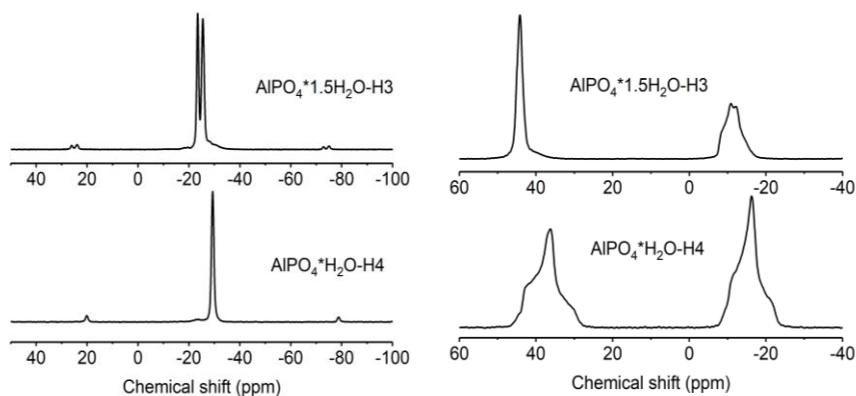


**Figure 3.**  $^{31}\text{P}$  MAS NMR (left) and  $^{27}\text{Al}$  MAS NMR (right) of  $\text{AlPO}_4 \cdot 1.5\text{H}_2\text{O} \cdot \text{H}_3$  (Lys-6) and  $\text{AlPO}_4 \cdot \text{H}_2\text{O} \cdot \text{H}_4$  (Lys-4).

cell of hydrated **APC** (Chart 2).<sup>27-28</sup> Lys-4 has only one tetragonal P peak at  $\delta = -29$  ppm, because in the monoclinic unit cell of  $\text{AlPO}_4 \cdot \text{H}_2\text{O} \cdot \text{H}_4$  there is only one unique P site (Chart 3).<sup>29</sup> The  $^{27}\text{Al}$  MAS NMR spectrum of Lys-6 has two peaks, the tetragonal Al at  $\delta = 42$  ppm, and the octahedral Al at  $\delta = -3$  ppm. The octahedral peak displays a shape of quadrupole distortion. The area ratio of both peaks is 1 to 1. Lys-4 has both tetrahedral and octahedra peaks of a 1 to 1 ratio, too. Both materials possess stoichiometric framework compositions according to the formula and structures.

Figure 4 shows the TG/DTA analysis of Lys-6 and Lys-4 samples.

Lys-6  $\text{AlPO}_4 \cdot 1.5\text{H}_2\text{O} \cdot \text{H}_3$  (**APC**) exhibits two endothermic weight losses, i.e., ca. 6% at  $70^\circ\text{C}$  and ca. 12% at  $130^\circ\text{C}$ . The first weight loss is attributed to the desorption of the water molecules in the 8-ring channel, and the second corresponds to the dehydration of the framework Al2 sites, accompanied by the phase transition to  $\text{AlPO}_4\text{-C}$  (**APC**). The stoichiometry is in accordance with the crystallographic composition. There is no further significant weight change that can be attributed to decomposition or combustion of the aminoacid. It means that no aminoacid molecules are occluded in the intracrystalline void space. Heat effects that are expected for phase transitions are not significant enough to be detected.

Lys-4  $\text{AlPO}_4 \cdot \text{H}_2\text{O}$ -H4 shows two approximately equal steps of dehydration at 180 and 250°C, respectively, each with ca. 6.4% weight loss. The material does not occlude aminoacids molecules, either.

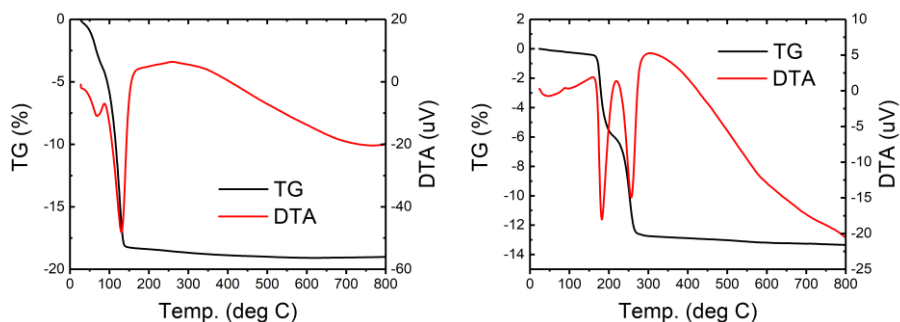


**Figure 4.** TG/DTA of  $\text{AlPO}_4 \cdot 1.5\text{H}_2\text{O}$ -H3 (left, Lys-6) and  $\text{AlPO}_4 \cdot \text{H}_2\text{O}$ -H4 (right, Lys-4).

The transformations of the crystalline phases of  $\text{AlPO}_4 \cdot 1.5\text{H}_2\text{O}$ -H3 (**APC**) upon heating in air atmosphere have been followed using *in situ* XRD (Figure 5). The heating rate was 10°C/min, with 5 min steps at every 50°C for recording the XRD patterns. The dehydration of  $\text{AlPO}_4 \cdot 1.5\text{H}_2\text{O}$ -H3 to  $\text{AlPO}_4$ -C occurs from 120°C; the pattern shows a ca. 1:1 mixture of both materials. The dehydration process lasts until 250°C, where  $\text{AlPO}_4$ -C is the major phase, and  $\text{AlPO}_4 \cdot 1.5\text{H}_2\text{O}$ -H3 is present as a trace impurity. At 300°C a further phase transition to  $\text{AlPO}_4$ -D happens. It completes at 400°C.  $\text{AlPO}_4$ -D is very stable up to 900°C, where its diffraction peaks start to decline in intensities. At 1000°C, about 1/2 intensities retain. The calcined sample remains as  $\text{AlPO}_4$ -D when it is cooled down to room temperature. The further transformations of  $\text{AlPO}_4$ -D to another  $\text{AlPO}_4$  phase at 650°C and collapse to  $\text{AlPO}_4$ -tridymite have been described by d'Yvoire,<sup>31</sup> and by Keller et al.,<sup>32</sup> have not been observed in the current experiment.

The phase transition of  $\text{AlPO}_4 \cdot \text{H}_2\text{O} \cdot \text{H}_4$  upon calcination is simple. It transforms into  $\text{AlPO}_4$ -cristobalite between 200 to 350°C, and further heating up to 1000°C improves its crystallinity (Figure S5).

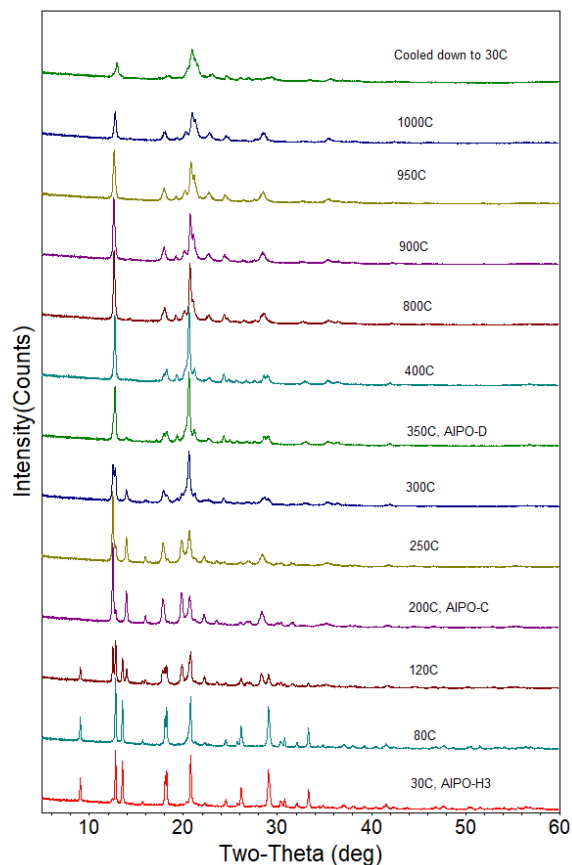


**Figure 5.** XRD patterns of  $\text{AlPO}_4 \cdot 1.5\text{H}_2\text{O} \cdot \text{H}_3$  (APC) heated up to 1000°C in ambient air.

**The role of aminoacids to the crystallization of  $\text{AlPO}_4 \cdot 1.5\text{H}_2\text{O} \cdot \text{H}_3$  (APC).**  $\text{AlPO}_4 \cdot 1.5\text{H}_2\text{O} \cdot \text{H}_3$  (APC) was synthesized previously using tetramethyl-ammonium hydroxide as SDA.<sup>27-28, 32</sup> It was also possible to crystallize without an organic SDA in aqueous HCl or  $\text{H}_2\text{SO}_4$  systems at pH ~ 5-6.<sup>33-34</sup> In the current study, three different aminoacid esters were added in the systems where  $\text{AlPO}_4 \cdot 1.5\text{H}_2\text{O} \cdot \text{H}_3$  (APC) crystallize at pH around 2. However, neither of the aminoacids was occluded in the intracrystalline void spaces of the product. This fact raises the question, if the aminoacids works merely as diffusion modifiers or pH modifiers rather than an SDA.

FTIR has been applied to track down the aminoacids in the initial gels and the crystalline products. Figure 6 shows the spectra of Pro-OMe·HCl, the mother liquor of the hydrogels that separated by high-speed centrifugation, the washed and freeze-dried gel solid, as well as the washed and dried  $\text{AlPO}_4 \cdot 1.5\text{H}_2\text{O} \cdot \text{H}_3$  (APC) product.

The mother liquor exhibits an almost identical spectrum as the aminoacid itself. There are no structured aluminum and phosphorous compounds to be recognized in the gel liquid.

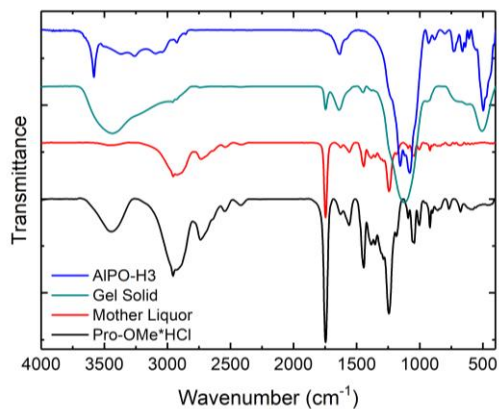


**Figure 6.** FTIR spectra of the Pro-OMe·HCl, the freeze-dried mother liquor, the washed and freeze-dried gel solids, and the crystalline products.

Interestingly, the washed gel solid, in addition to the broad bands at 1000, 1130 and 500  $\text{cm}^{-1}$ , which are the stretching and bending vibrations of the -T-O-T- chains of the oxidic aluminium and phosphorous species, shows unambiguous peaks of Pro-OMe, including C=O stretching at 1740  $\text{cm}^{-1}$ , C-N at 1240  $\text{cm}^{-1}$ , C-H at 2960 and 2900  $\text{cm}^{-1}$ , etc. Obviously, the gel solid is a composite of Pro-OMe and the amorphous and colloidal  $\text{AlPO}_4$ . The aminoacid – gel interaction is such that the cationic proline is not being washed out.

Furthermore, in the crystalline  $\text{AlPO}_4 \cdot 1.5\text{H}_2\text{O} \cdot \text{H}_3$  (**APC**), albeit occluded proline does not exist, vibrations corresponding to C-N stretching at 1240  $\text{cm}^{-1}$ , and C-H stretching at 2920 and 2850  $\text{cm}^{-1}$  are also visible. It is plausible to assign them to adsorbed proline on the crystal surfaces.

Figure S6 presents the FTIR spectra of His-OMe and Lys-OMe, the gel solids, as well as the  $\text{AlPO}_4 \cdot 1.5\text{H}_2\text{O} \cdot \text{H}_3$  (**APC**) and  $\text{AlPO}_4 \cdot \text{H}_2\text{O} \cdot \text{H}_4$  products. They show as well that the washed gel solids contain AA/ $\text{AlPO}_4$  composites and that the crystalline products possess surface C-N and C-H species.

Therefore, we justify the aminoacids do play an active role more than diffusion modifier or pH modifier during the crystallization of  $\text{AlPO}_4 \cdot 1.5\text{H}_2\text{O} \cdot \text{H}_3$  (**APC**) based on three arguments:

- 1) The  $\text{AlPO}_4 \cdot 1.5\text{H}_2\text{O} \cdot \text{H}_3$  (**APC**) phase did not crystallize in the blank experiments without aminoacids in the tested pH range.
- 2) The use of different aminoacids to prepare the initial gels results in the formation of  $\text{AlPO}_4 \cdot 1.5\text{H}_2\text{O} \cdot \text{H}_3$  (**APC**) phase at different pH.
- 3) The FTIR analysis evidenced the existences of stable aminoacid/ $\text{AlPO}_4$  composites in the gel solids, i.e., a strong interaction between the protonated aminoacid ester and the  $\text{AlPO}_4$  species has been

established (*vice versa*).

Summarizing the arguments, we elucidate the manner that the protonated aminoacid cation interacts with the solid part of the gel and actively participate in the crystallization process, as presented in Chart 4. These interactions can be summarized as follows: i) Structured composites of  $\text{AlPO}_4$  frameworks with the aminoacids ester capping the surfaces, populate on the gel/liquid interfaces, and initiate crystal growth; ii) The positively charged aminoacids ester on the surfaces of the growing crystals attracts the aluminate and phosphate anions from the aqueous phase. They exchange places so that the crystal grows a further layer, yet the surface is still capped by the aminoacids ester cation; iii) The consumed aluminate and phosphate in the aqueous phase are replenished through continuous dissolving of the gel solid. The mass exchange between the gel solid and liquid proceeds until the crystallization completes; and iv) Some aminoacids ester, therefore, remain adsorbed on crystal surfaces when the crystallization process completes.

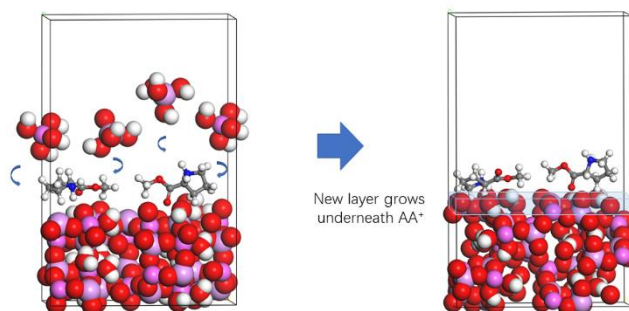


**Chart 4.** Schematic illustration of the crystal growth on the surface capped by protonated aminoacids ester cations.

This is a kind of non-typical structure-directing process where the adsorbed organic cations provide a dynamically charged surface, which exchanges places with the approaching nutrients for further crystal growth. This process differs from what we usually consider for the SDA role in the crystallization of zeolites where the SDA/framework composite stays intact and is continuously buried in the bulk when new crystal surfaces are growing. The role of aminoacids as a dynamic surface charge modifier is weaker than the traditional SDAs as a structure builder. Yet, it plays an active role in the formation of the framework  $\text{AlPO}_4$ . And it is stronger than merely diffusion or pH modifier.

## CONCLUSIONS

The zeotype framework material has been crystallized at the presence of three aminoacids ester at different pH, i.e., with Pro-OMe,  $\text{AlPO}_4 \cdot 1.5\text{H}_2\text{O} \cdot \text{H}_3$  (**APC**) crystallizes at pH = 2.0; His-OMe at pH = 2.3; Lys-OMe at pH = 2.5. Another framework material  $\text{AlPO}_4 \cdot \text{H}_2\text{O} \cdot \text{H}_4$  crystallizes with His-OMe at pH = 1.9; Lys-OMe at pH = 2.0. The crystalline phase appeared with Pro-OMe at pH = 2.4, but with  $\text{AlPO}_4$ -cristobalite impurity.

Characterization of the crystalline  $\text{AlPO}_4 \cdot 1.5\text{H}_2\text{O} \cdot \text{H}_3$  (**APC**) and  $\text{AlPO}_4 \cdot \text{H}_2\text{O} \cdot \text{H}_4$  proves that they possess

the expected structural integrity and stability that are in accordance with literature data. Furthermore, various physical-chemical methods reveal that the aminoacids esters are not occluded in the intracrystalline void spaces of the products, but FTIR evidences the existences of stable AA/AlPO<sub>4</sub> composites in the synthesis gels, and small amounts of adsorbed aminoacids in the crystalline products, probably on the surfaces.

Based on the experimental observations, we propose that the key intermediate in the crystallization process is the structured composite of the growing crystallite with the protonated aminoacids ester capping its surfaces. The charged surface cations attract the AlO<sub>4</sub><sup>-</sup> and PO<sub>4</sub><sup>-</sup>-building blocks and facilitating crystal growth. In this process, the aminoacids plays a particular, yet active structure-directing role, as surface charge modifiers of the growing crystals.

## SUPPORTING INFORMATION

A complete list of samples with synthetic recipes; further XRD patterns, SEM pictures and FTIR spectra that have been discussed in the paper, compiled in a PDF file.

## AUTHOR INFORMATION

### Corresponding Authors

**Valentin Valtchev** - Normandie University, ENSICAEN, UNICAEN, CNRS, Laboratoire Catalyse et Spectrochimie, F-14000 Caen, France; [orcid.org/0000-0002-2341-6397](https://orcid.org/0000-0002-2341-6397); Email: [valentin.valtchev@ensicaen.fr](mailto:valentin.valtchev@ensicaen.fr).

**Xiaobo Yang** - The ZeoMat Group, Qingdao Institute of Bioenergy and Bioprocess Technology, CAS, Laoshan District, CN-266101 Qingdao, China; [orcid.org/0000-0001-9373-8685](https://orcid.org/0000-0001-9373-8685); Email: [yangxb@qibebt.ac.cn](mailto:yangxb@qibebt.ac.cn).

### Authors

**Qiaolin Lang** - The ZeoMat Group, Qingdao Institute of Bioenergy and Bioprocess Technology, CAS, Laoshan District, CN-266101 Qingdao, China; [orcid.org/0000-0002-2674-584X](https://orcid.org/0000-0002-2674-584X).

**Guangying Fu** - The ZeoMat Group, Qingdao Institute of Bioenergy and Bioprocess Technology, CAS, Laoshan District, CN-266101 Qingdao, China

**Haonuan Zhao** - The ZeoMat Group, Qingdao Institute of Bioenergy and Bioprocess Technology, CAS, Laoshan District, CN-266101 Qingdao, China; Normandie University, ENSICAEN, UNICAEN, CNRS, Laboratoire Catalyse et Spectrochimie, F-14050 Caen, France

**Juan Wang** - The ZeoMat Group, Qingdao Institute of Bioenergy and Bioprocess Technology, CAS, Laoshan District, CN-266101 Qingdao, China

## Author Contributions

The manuscript was written through contributions of all authors. All authors have given approval to the final version of the manuscript.

## Notes

The authors declare no competing financial interest.

## ACKNOWLEDGMENT

The ZeoMat Group acknowledges the starting grant provided by QIBEBT. V.V. and X.Y acknowledge the collaboration in the framework of the Sino-French joint laboratory “Zeolites”.

## REFERENCES

1. Milton, R. M., Molecular Sieve Science and Technology. In *Zeolite Synthesis*, American Chemical Society: 1989; Vol. 398, pp 1-10.
2. Flanigen, E. M.; Patton, R. L.; Wilson, S. T., Structural, Synthetic and Physicochemical Concepts in Aluminophosphate-Based Molecular Sieves. In *Studies in Surface Science and Catalysis*, Grobet, P. J.; Mortier, W. J.; Vansant, E. F.; Schulz-Ekloff, G., Eds. Elsevier: 1988; Vol. 37, pp 13-27.
3. Vogt, E. T. C.; Whiting, G. T.; Dutta Chowdhury, A.; Weckhuysen, B. M., Chapter Two - Zeolites and Zeotypes for Oil and Gas Conversion. In *Advances in Catalysis*, Jentoft, F. C., Ed. Academic Press: 2015; Vol. 58, pp 143-314.
4. Flanigen, E. M., Chapter 2 Zeolites and molecular sieves: An historical perspective. In *Studies in Surface Science and Catalysis*, van Bekkum, H.; Flanigen, E. M.; Jacobs, P. A.; Jansen, J. C., Eds. Elsevier: 2001; Vol. 137, pp 11-35.
5. Flanigen, E. M., Molecular sieve zeolite technology - The first twenty-five years. *Pure & Applied Chemistry* **1980**, 52 (9), 21.
6. Li, Y.; Li, L.; Yu, J., Applications of Zeolites in Sustainable Chemistry. *Chem* **2017**, 3 (6), 928-949.
7. Zhang, Q.; Yu, J.; Corma, A., Applications of Zeolites to C1 Chemistry: Recent Advances, Challenges, and Opportunities. *Advanced Materials* **2020**, 32 (44), 2002927.
8. Li, Y.; Yu, J., Emerging applications of zeolites in catalysis, separation and host-guest assembly. *Nature Reviews Materials* **2021**.
9. Zaarour, M.; Dong, B.; Naydenova, I.; Retoux, R.; Mintova, S., Progress in zeolite synthesis promotes advanced applications. *Microporous and Mesoporous Materials* **2014**, 189, 11-21.
10. Breck, D. W., *Zeolite Molecular Sieves: Structure, Chemistry, and Use*. John Wiley and Sons: New York, London, Sydney, and Toronto, 1974; p 771.
11. Lobo, R. F.; Zones, S. I.; Davis, M. E., Structure-direction in zeolite synthesis. *Journal of inclusion phenomena and molecular recognition in chemistry* **1995**, 21 (1), 47-78.
12. Gómez-Hortigüela, L.; Cambor, M. Á., Introduction to the Zeolite Structure-Directing Phenomenon by Organic Species: General Aspects. In *Insights into the Chemistry of Organic Structure-Directing Agents in the Synthesis of Zeolitic Materials*, Gómez-Hortigüela, L., Ed. Springer International Publishing: Cham, 2018; pp 1-41.
13. Baerlocher, C.; McCusker, L. B.; Olson, D. H., Database of zeolite structures. [www.iza-online.org](http://www.iza-online.org).

14. Treacy, M.; Forster, M., Atlas of Prospective Zeolite Structures. <http://www.hypotheticalzeolites.net/>.
15. Chen, Z.; Zhang, J.; Yu, B.; Zheng, G.; Zhao, J.; Hong, M., Amino acid mediated mesopore formation in LTA zeolites. *Journal of Materials Chemistry A* **2016**, *4* (6), 2305-2313.
16. Zhang, J.; Chen, Z.; Wang, Y.; Zheng, G.; Zheng, H.; Cai, F.; Hong, M., Influence of the nature of amino acids on the formation of mesoporous LTA-type zeolite. *Microporous and Mesoporous Materials* **2017**, *252*, 79-89.
17. Hong, M.; Chen, Z. W.; Zhang, J.; Dong, L.; Wang, Y. D.; Chen, C.; Qian, W.; Wang, S. W.; Huang, Z. A.; Yuan, X. N., Synthesis and application of hierarchical zeolites prepared using amino-acid mesoporegens. *IOP Conference Series: Materials Science and Engineering* **2019**, *479*, 012113.
18. Davis, M. E., A Thirty-Year Journey to the Creation of the First Enantiomerically Enriched Molecular Sieve. *ACS Catalysis* **2018**, *8* (11), 10082-10088.
19. Brand, S. K.; Schmidt, J. E.; Deem, M. W.; Daeyaert, F.; Ma, Y.; Terasaki, O.; Orazov, M.; Davis, M. E., Enantiomerically enriched, polycrystalline molecular sieves. *Proceedings of the National Academy of Sciences* **2017**, *114* (20), 5101.
20. Tong, M.; Zhang, D.; Fan, W.; Xu, J.; Zhu, L.; Guo, W.; Yan, W.; Yu, J.; Qiu, S.; Wang, J.; Deng, F.; Xu, R., Synthesis of chiral polymorph A-enriched zeolite Beta with an extremely concentrated fluoride route. *Scientific Reports* **2015**, *5* (1), 11521.
21. Rigo, R. T.; Balestra, S. R. G.; Hamad, S.; Bueno-Perez, R.; Ruiz-Salvador, A. R.; Calero, S.; Cambor, M. A., The Si-Ge substitutional series in the chiral STW zeolite structure type. *Journal of Materials Chemistry A* **2018**, *6* (31), 15110-15122.
22. Nenoff, T. M.; Thoma, S. G.; Provencio, P.; Maxwell, R. S., Novel Zinc Phosphate Phases Formed with Chiral d-Glucosamine Molecules. *Chemistry of Materials* **1998**, *10* (10), 3077-3080.
23. Boekfa, B.; Pantu, P.; Limtrakul, J., Interactions of amino acids with H-ZSM-5 zeolite: An embedded ONIOM study. *Journal of Molecular Structure* **2008**, *889* (1), 81-88.
24. Stückenschneider, K.; Merz, J.; Hanke, F.; Rozyczko, P.; Milman, V.; Schembecker, G., Amino-Acid Adsorption in MFI-Type Zeolites Enabled by the pH-Dependent Ability to Displace Water. *The Journal of Physical Chemistry C* **2013**, *117* (37), 18927-18935.
25. Addadi, L.; Weiner, S., Biomineralization: mineral formation by organisms. *Physica Scripta* **2014**, *89* (9), 098003.
26. Fromm, H. J.; Hargrove, M. S., Introduction to Biomolecules. In *Essentials of Biochemistry*, Fromm, H. J.; Hargrove, M., Eds. Springer Berlin Heidelberg: Berlin, Heidelberg, 2012; pp 5-34.
27. Pluth, J. J.; Smith, J. V., A hydrated aluminophosphate with both 4.8<sup>2</sup> and 6<sup>3</sup> sheets in the 4-connected framework. *Nature* **1985**, *318* (6042), 165-166.
28. Pluth, J. J.; Smith, J. V., Hydrated aluminophosphate (AlPO<sub>4</sub>·1.5H<sub>2</sub>O) with PO<sub>4</sub>, AlO<sub>4</sub> and AlO<sub>4</sub>(H<sub>2</sub>O)<sub>2</sub> groups and encapsulated water. *Acta Crystallographica Section C* **1986**, *42* (9), 1118-1120.
29. Poojary, D. M.; Balkus, K. J.; Riley, S. J.; Gnade, B. E.; Clearfield, A., Synthesis and ab initio structure determination of AlPO<sub>4</sub>·H<sub>2</sub>O·H<sub>4</sub> from powder diffraction data. *Microporous Materials* **1994**, *2* (4), 245-250.
30. Kniep, R.; Mootz, D.; Vegas, A., Variscite. *Acta Crystallographica Section B* **1977**, *33* (1), 263-265.
31. d'Yvoire, F., Etude des phosphates d'aluminium et de fer trivalent. I. L'orthophosphate neutre d'aluminium. *Bull. Soc. Chim. France* **1961**, 1762-1776.
32. Keller, E. B.; Meier, W. M.; Kirchner, R. M., Synthesis, structures of AlPO<sub>4</sub>-C and AlPO<sub>4</sub>-D, and their topotactic transformation. *Solid State Ionics* **1990**, *43*, 93-102.
33. Kunii, K.; Narahara, K.; Yamanaka, S., Template-free synthesis and adsorption properties of microporous crystal AlPO<sub>4</sub>-H<sub>3</sub>. *Microporous and Mesoporous Materials* **2001**, *50* (2), 181-185.
34. Lagno, F.; Demopoulos, G. P., Synthesis of Hydrated Aluminum Phosphate, AlPO<sub>4</sub>·1.5H<sub>2</sub>O (AlPO<sub>4</sub>-H<sub>3</sub>), by Controlled Reactive Crystallization in Sulfate Media. *Industrial & Engineering*

*Chemistry Research* **2005**, *44* (21), 8033-8038.